Decolourization of Crystal Ponceau 6R dye by coagulation-flocculation process: Investigation of operation parameters and polymer adsorption studies

I.A Obiora-Okafo[1], O.D Onukwuli[2]
[1]Department of Chemical Engineering, Madonna University, Elele, Nigeria
[2]Department of Chemical Engineering, Nnamdi Azikiwe University, Awka, Nigeria

Abstract: Recent advance on the application of natural polymer coagulants in coagulation-flocculation process has attracted a widespread interest. Previous research has demonstrated that plant-based coagulants could enhance the performance of the coagulation-flocculation process. In this research, performance of these natural polymer coagulants; Vigna unguiculata coagulant (VUC), Telfairia occidentalis coagulant (TOC), Brachystegia eurycoma coagulant (BEC), Vigna subterranean coagulant (VSC) and Moringa oleifera coagulant (MOC) for colour removal from crystal Ponceau 6R dye were investigated. The influences of operational parameters such as pH, coagulant dosage, dye concentration, settling time and temperature have been tested and the optimum operating range for each operating variables were experimentally determined. The maximum percentage removal for the parameters studied was 96.04%, 94.7%, 94.50%, 94.22% and 93.3% for BEC, VSC, MOC, TOC and VUC, respectively. Charge neutralization, adsorption, chain bridging of particles and sweep-flocculation mechanisms all played roles in the colour removal process. Adsorption of contaminant particles on the polymer surfaces occur mostly as a monomolecular layer and mostly according to the mechanism of chemisorption. Polymer adsorption kinetics data as described mostly by the pseudo-second order and Elovich model with high correlation ($R^2 > 0.925$) confirms coagulation-flocculation/adsorption process behaving more as a second-order rate process and that the overall adsorption rate process mostly controlled by chemisorption.

Keywords: **Coagulation-flocculation, Crystal Ponceau 6R, colour removal, polymer coagulants, polymer adsorption.**

I. INTRODUCTION

Coagulation-flocculation process in recent studies have been found not only to remove suspended solids from water, but also reduces organic and inorganic compounds from different wastewater sources such as dye containing wastewater, textile wastewater, municipal sewage, micro-polluted water, oily wastewater, pulp and paper industries [1, 2]. Colour is one of the contaminants found in industrial wastewater, and has been effectively removed using coagulation-flocculation technique [2, 3]. Studies on improving the performance of coagulation-flocculation process have attracted a lot of attention.

Its performance is largely affected by the type of coagulant used. A good choice of coagulant enhances the aggregation of particles for large flocs formation capable of rapid settling through charge neutralization, enmeshment in a precipitate, double layer compression, interparticle bridging, and electrostatic patch and adsorption mechanisms. These mechanisms of particles flocculation are better experienced because natural polyelectrolytes of high molecular weight are used as coagulants. Therefore, research on wastewater treatment has been refocused on the use of new natural coagulants (organic polymers) to improve the coagulation-flocculation process [4]. Natural organic polymers may be anionic, cationic or non-ionic in nature and are collectively termed polyelectrolyte due to their ionic nature. A comprehensive account of water-soluble polyelectrolyte coagulants has been given by Bolto and Gregory [5].

Natural polymer coagulants are concerned to many researchers because of their abundant source, cost effective, environment friendly, multifunction, and biodegradable in water purification. Mechanisms of particles flocculation by natural polymers could be describe by charge neutralization, sweep-flocculation, interparticle bridging, and electrostatic patch mechanisms. These mechanisms are all dependent on the polymer adsorption of particles on the polymer surfaces. Polymer adsorption occurs when there are some affinity between polymer segments and particle surfaces. Adsorption interactions are possible by electrostatic interaction, hydrogen bonding and ion bonding [5]. Electrostatic interaction occurs when polyelectrolytes with a charge opposite to that of the surface (cationic polyelectrolytes on negative surfaces) absorb strongly, simply because of attraction between opposite charge ionic groups. Hydrogen bonding occurs when polymers adsorb on surfaces with suitable hydrogen bonding sites. Ion bonding occurs when anionic polyelectrolytes are adsorbed on negatively-charged surfaces, despite electrostatic repulsion.

The efficacies of using these plant seeds: Cowpea seed (*Vigna unguiculata*), Fluted pumpkin seed (*Telfairia occidentalis*), Black Timber seed (*Brachystegia*

eurycoma), Bambara nut seed (*Vigna subterranean*) and Horse radish seed (*Moringa oleifera*), as plant-based cationic coagulants have been studied here. The use of these plant-based precursors was established because animal-based precursors are expensive and difficult in sourcing [6]. Crude extract from the seeds is believed to be a soluble cationic protein and have showed the ability to act as a natural polymer coagulant [7-12]. These Plant-based polymer coagulants employed in this study have not been utilized in the decolourization of Crystal Ponceau 6R dye.

In the present study, the potentials and performances of natural coagulants were studied for colour removal from Crystal Ponceau 6R dye (Acid Red 44). The influence of pH, coagulant dosage, dye concentration, settling time and temperature on the coagulation-flocculation process was investigated and the optimal conditions were obtained. Polymer adsorption studies were done extensively following adsorption capacity, adsorption isotherms and adsorption kinetics.

II. MATERIALS AND METHODS

A. Preparation of Coagulants

Dry seeds of five samples were bought from local market of Enugu city, Nigeria. Matured seeds showing no signs of discolouration, softening or extreme desiccation were used. The seeds were removed from the pod, dried under sun, and the external shells were removed. The seeds kernels were ground to fine powder (63-600μm) using an ordinary food processor. The seed powder was then used in each experiment.

B. Extraction of Active Component

The seed kernels were ground to fine powder of approximate size 600μm to achieve solubilisation of active ingredients in the seeds. The active component from coagulants was extracted by adding distilled water to the fine powder to make 2% suspension (2g of fine powder fined samples in 100ml water). The suspension was stirred using a magnetic stirrer for 20 min at room temperature to accomplish extraction and then filtered through a rugged filter paper (Macherey Nagel, MN 651/120). The resultant filtrate solutions were used as coagulants. Fresh solutions were prepared daily and kept refrigerated to prevent any ageing effects (such as change in pH, viscosity and coagulation activity). Also solutions were shaken vigorously before use. Fresh coagulants were prepared and used immediately for each sequence of experiment. The extractive method employed in obtaining the coagulating agents is a suitable and it also helps in sludge load reduction.

C. Characterization of the Coagulants

Moisture, protein, crude fat, crude fibre and ash contents of the seed powders were determined by the standard official methods of analysis of the A.O.A.C [13], while carbohydrate content was calculated by difference.

D. Buffered Solution

All assays were done in a pH-stable medium. Buffered solutions (pH 2, 4, 6, 7, 8, 10 and 12) were prepared by the standards established according to the National bureau of standards (NBS, US) and were standardized using a digital pH meter. All reagents used were of analytical purity grade.

E. Decolourization Procedures

1. Absorption spectrum and stock solutions preparation

Acid Red 44 (water soluble dye) was provided by May & baker England with a molecular structures as shown in Fig. 1. The characteristics of Acid Red 44 are summarized in Table 2. Dye with commercial purity was used without further purification. The absorption spectrum of the dye was obtained as follows by dissolving 1000mg/L of Acid Red 44 (AR 44) in distilled water. A sample of the solution was scanned against the blank of distilled water in the range of 200-850nm using UV-Vis spectrophotometer (Shimadzu, Model UV-1800). A maximum absorption spectrum was obtained against its reagent blank. Stock solution of 1000mg/ L of dye was prepared by dissolving accurately weighed amounts of AR 44 in separate doses of 1L distilled water. The desirable experimental concentrations of 10-100mg/L were prepared by diluting the stock solution with distilled water when necessary. The wavelength of maximum absorbance (λmax) and its calibration curves at λmax of the dye was determined.
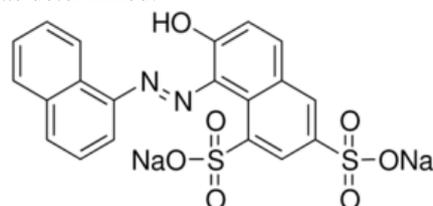

Fig 1. Structure of Crystal Ponceau 6R dye (Acid Red 44).

Table 1. Physical properties of Crystal Ponceau 6R dye.

Property	Data
Chemical name	Crystal Ponceau
Chemical formula.	$C_{20}H_{12}N_2\ O_7\ S_2\ Na_2$.
Molecule Weight (g/mol)	502.43
CAS number	2766 -77 - 0
EC number	E 126
UV/Visible Absorbance	Max (water): 511 +6nm
C.I number	16250
Class	AZ0
C.I name	Acid Red 44.

2. Decolourization determination

Colour measurement was determined with standard dilution multiple method (Wei, 2002) and by comparing absorbance to a calibration curve. AR 44 dye decolourization was determined by monitoring the

decrease in the absorbance peak at the maximum wavelength of 511nm. Dye concentration of the supernatant (from coagulation experiment) was measured using UV-Vis spectrophotometer (Shimadzu model 1800) at wavelength corresponding to the maximum absorbance (λmax) of the dye. The study was conducted by varying few experimental parameters which were pH, coagulants dosages, Initial dye concentrations, settling time and temperature. The pH was adjusted to the desired value using 0.1 M HCL and 0.1 M NaOH.

F. Coagulation studies

The jar test was performed to evaluate the performance of the coagulants agent extracted from the various processes as described above based on standard methods [14-16]. A set of beakers was used to simulate the coagulation-flocculation process. Each beaker contained 250ml of the dye solution. The coagulation-flocculation procedure involved 4min of rapid mixing at 100rpm. The mixing speed was reduced to 40 rpm for another 25 min. All the suspensions were left for settling (30-540 min). The additional centrifuging (5000rpm for 5min) was performed to obtain clear liquid for all samples before analysis. After settling, supernatant sample was withdrawn for absorbance analysis using UV-Vis spectrophotometer (Shimadzu model 1800) at maximum wavelength corresponding to the maximum absorbance of 511nm. Colour removal was measured as a decrease in optical density measurement at 511nm. Removal efficiency of colour was obtained according to the formula given below:

$$\text{Colour removal (\%)} = \left(\frac{C_0 - C}{C_0}\right) \times 100 \quad (1)$$

Where C_0 and C are the initial and final colour concentration (mg/L) in dye solutions before and after coagulation-flocculation treatment, respectively.

G. Polymer Adsorption Studies
1. Polymer adsorption capacity

The parameter extensively used in adsorption processes is the adsorption capacity (q). Contaminant removal by coagulation-flocculation occurs in two stages for all the mechanisms applied. For example the first mechanism charge neutralization, there is destabilization of colloids which may be governed by chemical interactions between molecules of the coagulants (cationic, positively charged) and of the contaminant (anionic, negatively charged). Then, once the coagulants-contaminant complex is formed, flocs begin to grow by sorption mechanisms. This should be the controlling stage, so that the entire process can be simulated as an adsorption phenomenon. Previous studies have found the coagulation capacity q to be a suitable evaluation parameter [4]. Polymer adsorption capacity (qt) at any time was determined according to the following equation (2):

$$q_t \text{ (mg/g)} = \frac{(C_0 - C_t)\, V}{M} \quad (2)$$

Where C_o is the initial contaminant concentration (mg/L), C_t is the contaminant concentration at time t in the bulk solution (mg/L), V is the volume of solution (L), and M is the coagulants mass (mg/L).

2. Polymer adsorption isotherm theory

An isotherm is the relationship that shows the distribution of adsorbate between the adsorbed phase and the solution phase equilibrium. The capacity of the polymers used is described by its equilibrium adsorption isotherm, which is characterized by certain constants whose values express the surface properties and affinity of the adsorbent. The purpose of the adsorption isotherms is to relate the adsorbate concentration in the bulk and the adsorbed amount at the interface [17]. Four adsorption models were analyzed in the present work: Langmuir, Freundlich, Temkin and Dubinin-Radushkevich isotherm models.

Langmuir model is based on the assumption that that each of these sites being capable of adsorbing one molecule, resulting in a monolayer-one molecule thick over the entire surface. The maximum adsorption occurs when the surface is covered by a monolayer of adsorbate [18]. The linear form Langmuir isotherm equation is given as:

$$\frac{C_e}{q_e} = \frac{1}{q_{max} K_L} + \frac{1}{q_{max}} C_e \quad (3)$$

Where, qmax is the maximum capacity (mg of contaminant/g of coagulants) for complete monolayer adsorption and KL (L/mg) is Langmuir adsorption constant. The essential characteristics of Langmuir equation can be expressed in terms of dimensionless separation factor, RL, defined as [19];

$$R_L = \frac{1}{1 + K_L C_0} \quad (4)$$

Where CO (mg/l) is the highest initial concentration of the adsorbent. Whereas RL value implies the adsorption to be unfavourable (RL>1), linear (RL=1) favourable (0<RL<1), or irreversible (RL= 0).

Freundlich model is based on sorption on a heterogeneous surface of varied affinities [20]. The linear form of Freundlich isotherm is given as:

$$\ln q_e = \frac{1}{n} \ln C_e + \ln K_F \quad (5)$$

Where KF (mg/g (l/mg) 1/n) is a Freundlich constant that indicates the sorption capacity of the polymer. n is a Freundlich adsorption order (dimensionless) that represents the parameter characterizing quasi-Gaussian energetic heterogeneity of the adsorption surface [21]. In general, n>1 suggest that contaminants are favourably

adsorbed on the polymer surfaces. The higher the n value the stronger the adsorption intensity.

Temkin model was derived from Langmuir adsorption isotherm by inserting the condition that the heat of adsorption decreases linearly with surface coverage [22]. Temkin model is expressed in Eq. 6 as:

$$q_e = \left(\frac{RT}{b_T}\right) \ln (AC_e) \qquad (6)$$

where $RT/b_T = B$ (J/mol), which is the Temkin constant related to the heat of sorption, whereas A (l/g) is the equilibrium binding constant corresponding to the maximum binding energy. R (8.314J/mol k) is the universal gas constant and T (K) is the absolute solution temperature.

Dubinin-Radushkevich model [23] is generally applied to express the adsorption mechanism with a Gaussian energy distribution over the heterogeneous surface. Dubinin-Radushkevich isotherm has been used in the linear form of:

$$\ln q_e = \ln q_m - \beta\varepsilon^2 \qquad (7)$$

Where q_e (mg/g) is the equilibrium solid phase concentration, q_m is the theoretical saturated capacity, ε is the Polanyi potential given as:

$$\varepsilon = RT \ln \left(1 + \frac{1}{C_e}\right) \qquad (8)$$

β is a constant related to the adsorption energy by the Eq. (9):

$$E = (2\beta)^{-1/2} \qquad (9)$$

Where E (sorption mean free energy which is the energy required to transfer one mole of the contaminant from infinity in solution to the surface of solid. R is the gas constant (8.314 $Jmol^{-1}K^{-1}$) and T is the temp (K).

3. Polymer adsorption kinetics theory

Adsorption kinetic provides an invaluable insight into the controlling mechanism of adsorption processes which in turn governs mass transfer and the residence time [24]. The kinetic data were analyzed using pseudo-first order, pseudo-second order, Elovich and intraparticle diffusion model. Lagergren proposed pseudo-first order kinetic equation [25]. In the form of:

$$\text{Log} (q_e - q_t) = \log q_e - \frac{K_{f1}}{2.303t} \qquad (10)$$

Where q_t is the amount of adsorbate adsorbed at time t (mg/g), q_e the adsorption capacity at equilibrium (mg/g), k_{f1} the pseudo-first order rate constant (min^{-1}), and t is the time (min). The value of the adsorption rate constant, k_{f1}, for the dye was determined from the plot of log $(q_e - q_t)$

against t. Pseudo-second order equation [26] predicts the behaviour over the whole range of adsorption with chemisorptions being the rate controlling step and it is represented by:

$$\frac{t}{q_t} = \frac{1}{k_2 q_e} + \frac{1}{q_e} t \qquad (11)$$

where k_2 is the pseudo-second order rate constant ($gmg^{-1}min^{-1}$). The linear plot of $\frac{t}{q_t}$ versus t will give $\frac{1}{q_e}$ as the slope and $\frac{1}{k_2 q_e}$ as the intercept. The initial adsorption rate h ($mg^{-1} min^{-1}$) at t = 0 is defined as follows [27]:

$$h = k_2 q_e^2 \qquad (12)$$

q_e is obtained from the slope of $\frac{t}{q_t}$ versus t and k_2 from the intercept. h is obtained from the Eq. (12). Elovich [28] kinetic model equation, one of the most useful methods describing chemisorptions processes, is defined as;

$$q_t = \frac{1}{\beta}\ln(\alpha\beta) + \frac{1}{\beta} \ln t \qquad (13)$$

where α ($mgg^{-1}min^{-1}$) is the initial sorption rate and β (gmg^{-1}) is related to the extent of surface coverage and activation energy for chemisorptions. The value of $\left(\frac{1}{\beta}\right)$ is indicative of the available number of sites for adsorption while $\frac{1}{\beta} \ln(\alpha\beta)$ is the adsorption quantity when ln t = 0. Intraparticle diffusion model [29] was calculated in order to gain insight into the mechanisms and rate controlling steps affecting the kinetics of adsorption. The model is expressed as:

$$q_t = k_3 t^{1/2} + C \qquad (14)$$

Where k3 is the intraparticle diffusion rate constant (mgg-1min-1/2) and C is the intercept. k3 and C can be evaluated from the intercept and slope of the plot of qt versus t½. The value of C relates to the thickness of the boundary layer. The large C implies the greater effect of the boundary layer [30].

The suitability of the kinetic model to describe the adsorption process was validated by the normalized standard deviation, Δq (%) given by:

$$\Delta q \, (\%) = 100 \sqrt{\frac{\sum\left[(q_{exp} - q_{cal})/q_{exp}\right]^2}{df}}$$

Where, d_f is the degrees of freedom of the fitting equation. The number of degree of freedom as follows N-n_p, where N is the number of data points and n_p is the number of parameters. q_{exp} (mg/g) and q_{cal} (mg/g) are the

experimental and calculated adsorption capacities, respectively.

III. RESULTS AND DISCUSSION

A. Characterization Result

The proximate analysis of coagulant precursors were determined and summarized in Table 2. The study shows a high protein contents. The results obtained from the proximate composition as shown in Table 2 also agrees with the literature results that the active coagulating agents are diametric cationic peptides, which are capable of destabilizing the anionic dye particles. It justifies the use of these coagulants as potential source of coagulant in this work.

Table 2. Proximate compositions determination of the coagulant precursor

| S/No.	Parameters	Values				
		Vigna unguiculata (Cowpea)	Telfaria occidentalis (fluted pumpkin seed)	Brachystegia eurycoma (Black timber)	Vigna subterranean (Bambara nut)	Moringa oleifera seed
1	Yield	11.5	38.4	28.31	14.6	32.68
2	Bulk density (g/mL)	0.299	0.354	0.235	0.241	0.425
3	Moisture Content (%)	9	12.58	7.25	10	5.02
4	Ash content (%)	3.48	1.52	3.48	2.97	2.12
5	Protein content (%)	25.14	55.09	19.77	18.15	39.34
6	Fat content (%)	0.53	17.17	10.53	6.3	19.47
7	Fibre content (%)	6.78	0.87	2.2	1.64	1.16
8	Carbohydrate (%)	55.07	12.77	56.76	60.94	32.89

B. Absorption Spectra of Dye and Calibration Curve Analysis

Figure 2 records the electronic absorption spectra of 1000mg/L stock solution of AR 44 in the wavelength range of 250-800nm. The maximum wavelength (λ_{max}) of AR 44 obtained was 516nm. The λ_{max} values obtained from the spectra analysis were in agreement with the standard values obtained in the literature. The absorbance or calibrated curve carried at different initial dye concentrations of 10-100 mg/L for AR 44 was obtained as shown in Fig 3. Beer-Lambert's law was obeyed in the desired concentration range following the straight line graphs obtained from the plots [31]. The result of the calibration analysis validated spectrophotometric method as the most accurate method for determining the concentrations of colour in aqueous solution.
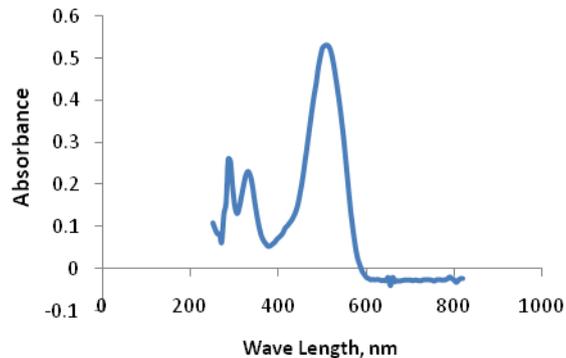
Fig 2. Spectrum Peak Report for AR44
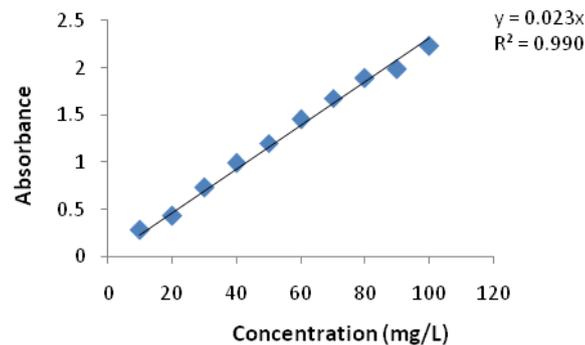
Fig 3. Calibration curve for AR 44 at wave length of 511 nm

C. Effects of Process Parameters in Decolourization Procedure

1. Effect of pH

pH plays an important role in the coagulation-flocculation process and must be controlled to establish optimum conditions for process. The effectiveness of the polymers in removing colour from AR 44 dye is highly dependent on pH as shown in Fig. 4. The polymers showed higher colour removals at low pH values and maximum removal was obtained when initial pH of the solutions were 2. In other words, colour removal efficiency decreased with increasing pH. The highest removal efficiency was observed in MOC followed by VUC giving efficiencies of 92.1% and 91.7%, respectively. Charge on the hydrolysis products and precipitation of polymeric hydroxides are both controlled by pH variations [32]. As the functional groups of the acid dyes are anionic, hydrolyses products of the organic biopolymer can neutralize the negative charges on dye molecules followed by polymer adsorption. Charge neutralization, sweep coagulation-flocculation and

polymer adsorption played a predominant role in the coagulation-flocculation process due to its pH value. Generally, adsorption of the natural organic contaminants (NOC) or NOC-polymer contaminant complexes onto polymer hydroxide precipitate forming at high pH is also limited. As pH increases, natural organic compounds become more negatively charged and polymer hydrolysis species become less positively charged, resulting in less adsorption propensity. For these reasons, coagulation-flocculation of NOC in wastewater is mainly performed under low pH conditions along with the presence of soluble cationic polymer hydrolysis species. These species react with anionic functional groups on NOC to precipitate as a polymer-NOC. Conclusively, high removal efficiency at low pH values are predominant in organic contaminants removal from acid dyes. Similar results were reported by [1, 4, 33].
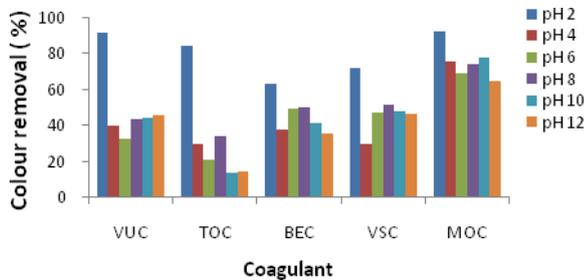

Fig 4. Effect of PH on the colour removal (%) using polymer coagulants IDC=100mg/L, coagulant dosage=600 mg/L, settling time=360 min, temperature=303K
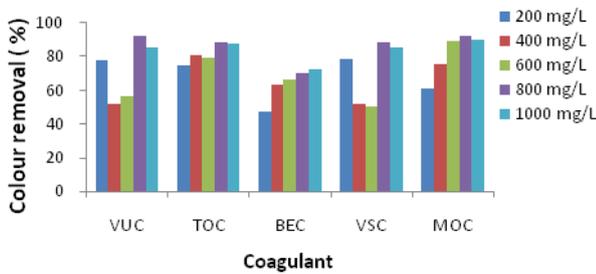

Fig 5. Effect of coagulant dosage on the colour removal (%) using polymer coagulants IDC=100mg/L, PH=2, settling time=360 min, temperature=303K
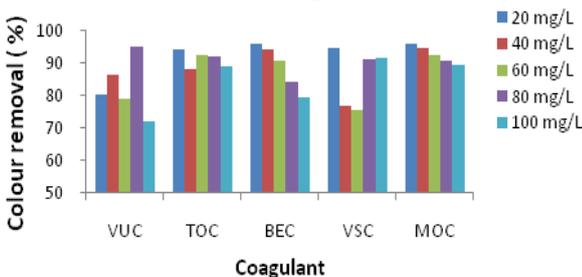

Fig 6. Effect of initial dye concentration on the colour removal (%) using polymer coagulants PH=2, settling time=360 min, temperature=303K
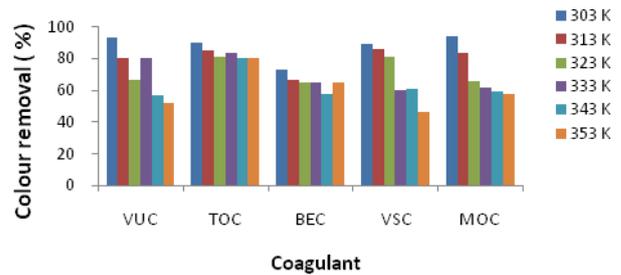

Fig 7. Effect of temperature on the colour removal (%) using polymer coagulants PH=2, IDC=20 mg/L, temperature=303K

2 Effect of coagulant dosages

Figure 5 shows the effect of coagulant dosages on colour removal efficiencies for different polymer coagulants. The result illustrated in Fig. 5 (AR 44) indicates that with the increase of coagulant dosages, the removal efficiencies increased and maximum removal efficiency was achieved at coagulant dosages (800 mg/L) with MOC efficiency of 92.2% followed by VUC with efficiency of 91.9%. The high removal efficiencies of >70% found in all the coagulants for the 800 mg/L doses confirms that sweep-flocculation and adsorption mechanism was observed to be predominant mechanism in the colour removal. With the increase of coagulant dosages, the removal efficiency steadily increased and no "re-stabilization zones" with negative dye removals were found even at the applied maximum dosage (800 mg/L). The coagulant apparently served as condensation nuclei and the dye particles were enmeshed as the precipitate was settled. The high dosages of the organic polymer could also give rise to chain bridging and adsorption mechanism [1].

More increase in the coagulant dosages resulted in a decrease in the removal efficiency. This trend was observed in Fig. 5, at dosages higher than 800mg/L, when the removal efficiencies began to decrease. This implies that overdosing happened in the reaction solution. Overdosing deteriorates supernatant quality, referring to the "re-stabilization" of the colour particles and therefore the particles could not coagulate well. With excess polymer adsorption, the particle charge may be reversed.

3. Effect of initial dye concentration

The concentration of dye provides an important driving force to overcome all the mass transfer resistance of the dye between the aqueous and solid phases [34]. The effect of initial dye concentration on the colour removal efficiency at different coagulants and their optimum doses is shown in Fig. 6. From Fig. 6, dye concentrations slightly have a significant effect on colour removal efficiency. This indicates that it also plays an important role in the coagulation-flocculation process. Highest efficiency was observed at 20 mg/L for BEC with

removal efficiency of 96.0% the least removal was at 60mg/L VSC with removal efficiency of 75.6%.
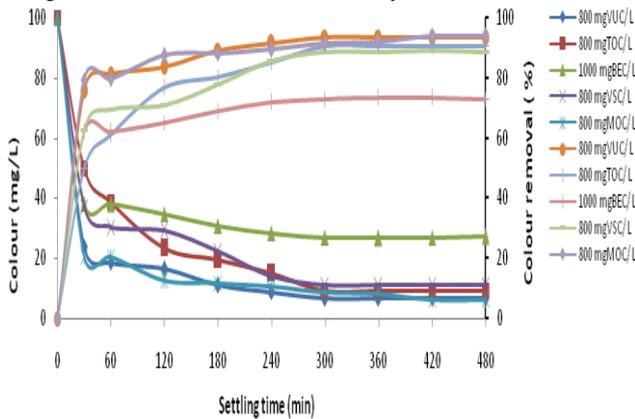
Fig 8. Kinetics of colour removal and effect of seetling time on the colour removal (%) using polymer coagulants PH=2, IDC=20 mg/L, temperature=303K

4. Kinetics of colour removal and effect of settling time on the percentage colour removal.

The effect of coagulation-flocculation was analyzed at different time at optimum dosage and pH of VUC, TOC, BEC, VSC, and MOC. Floc formation involves both interactions of coagulant hydroxide precipitate following hydrolyses reaction and contact with particles. Coagulation-flocculation performance is usually evaluated through time-dependent decrease in particle concentration. This decrease in the concentration of particles coincides with the growth of aggregates.

Figure 8 shows the kinetics effect of colour concentration and removal efficiencies of colour over settling time for AR 44. As shown in Fig. 8, the highest reduction in concentration was observed in 800mgVUC/L followed by 800mgMOC/L resulting in removal efficiencies of 93.5% and 91.9% respectively. The lowest reduction was observed in 1000mgBEC/L with removal efficiency of 73.3%. Over 75% of colour was removed within 30min in both 800mgVUC/L and 800mgMOC/L. This rapid reduction indicates a rapid coagulation-flocculation process. This is probably because of complex coagulation-flocculation mechanisms that may involve a net-like structure formation, which does not need a very long time. The coagulation-flocculation process for colour removal generally, was a bit fast at onset resulting to over 65% removal within 120 min of coagulation-flocculation. The longer coagulation-flocculation time is also a confirmation of presence of sorption mechanism. The reduction concentration did not vary significantly after 300 min from the initial stage. This shows that equilibrium can be assumed to have been achieved after 300 min. Destabilization of the aggregate flocs could set in after this time. This basically due to saturation of the active sites which does not allow further polymer adsorption and also prolonged settling time.
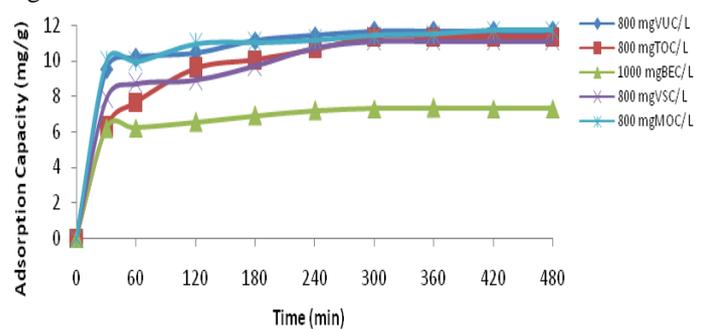
5. Effect of temperature on the colour removal efficiency

Figure 7 shows the effect of temperature on contaminants removal efficiency. General observation can be deduced from the plot that as temperature increases colour removal efficiency decreases. The temperature that gave highest removal efficiencies was 303K. This trend could be as a result of high solution temperature breaking polymer chains, reducing the surface adsorption sites of the coagulants. Also high temperature reduces the flocs growth which in turn reduces coagulation-flocculation process.

D. Polymer Adsorption Results

1. Polymer adsorption capacity for colour removal from dye wastewater.

The effect of settling time on the polymer adsorption capacity for colour at different coagulants and optimum doses is shown in Fig. 9. This figure shows that the adsorption capacity for colour increases with increase in settling time. From Fig. 9, the maximum adsorption capacity of 11.72mg/g is obtained at 420min, 800mgMOC/L. The plot of adsorption capacity clearly shows that there was a rapid increase in adsorption capacity during the first 60min. The fast adsorption at the initial stage may be due to the higher driving force (contaminants concentration) making fast transfer of particles from the bulk of contaminant region to the polymer surface. Also, due to high avalability of the uncovered surface area and remaining active sites of the coagulants.

Fig 9. Effect of cogulant dosage and seetling time on coagulation sorption for AR 44 colour removal PH=2, IDC=20 mg/L, temperature=303K

2. Polymer adsorption isotherm

Figure 10-13 shows the Langmuir, Freundlich, Temkin and D-R isotherm plots. Table 3 summarizes all the constants and correlation coefficient (R^2) values obtained from the isotherm models applied for the polymer adsorption of colour on the coagulants. From the table, the Langmuir model yielded highest values of the correlation coefficient R^2 (>0.991) compared to Freundlich models, indicating a monolayer adsorption mechanism. Isotherm studies show that adsorption of contaminant particles on the polymer surfaces occurred more according to the mechanism of chemisorption which

involves sharing of electrons between the adsorbate molecules and the surface of polymer resulting in a chemical reaction. The values of R_L and n obtained gave a favourable colour adsorption onto polymer surfaces.
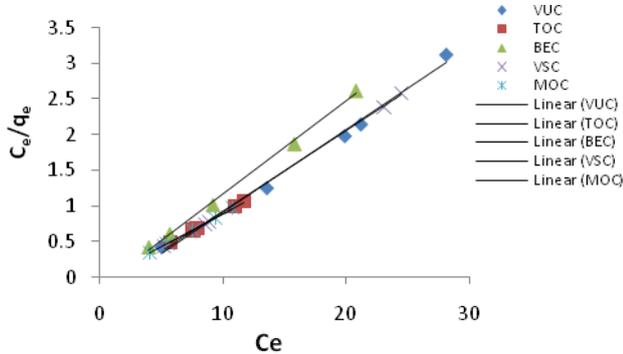

Fig 10. Langmuir isotherm for colour removal from AR 44 dye at 303K.
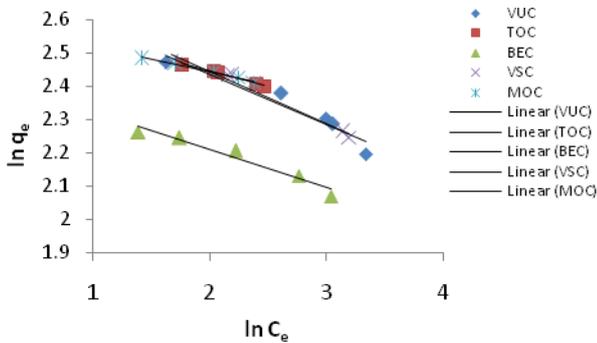

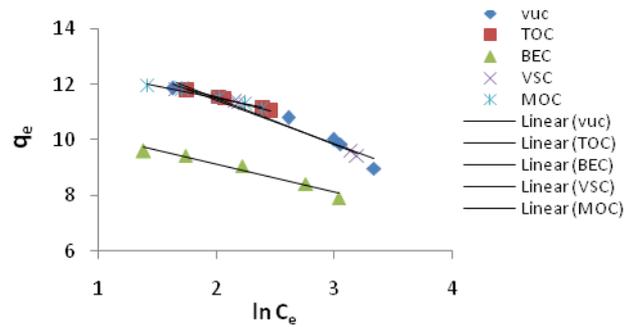Fig 11. Freundlich isotherm for colour removal from AR 44 dye at 303K.

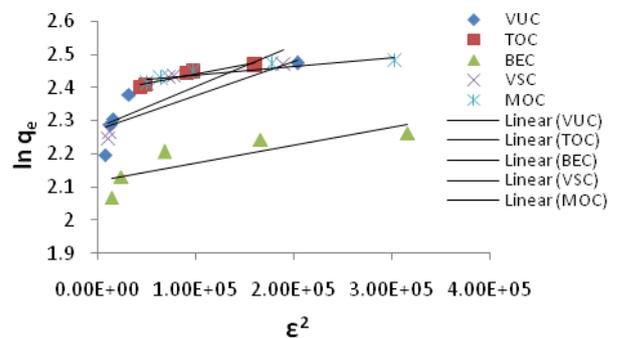Fig 12. Temkin isotherm for colour removal from AR 44 dye at 303K.

Fig 13. D-R adsorption isotherm for colour removal from AR 44 dye at 303K.

Table 3. Langmuir, Freundlich, Temkin and D-R isotherm parameters for adsorption mechanism studies on the colour removals from AR 44.

| Polymers	Langmuir				Freundlich			Temkin			D - R			
	q_{max} (mg L/mg)	K_L (L/mg)	R_L^2	R_L	K_f (mg/g(L/mg)$^{1/n}$)	n	R_F^2	A (L/mg)	B	R_T^2	q_m (mol/ g)	β (mol^{2}K J^{-2})	R_{D-R}^2	E (KJmol^{-1})
VUC	9.09	0.44	0.991	0.022	15.44	6.67	0.919	9.8E-05	-1.58	0.941	9.68	1E-06	0.701	707.11
TOC	10.42	1.33	0.999	0.008	13.93	10.8	0.988	2.7E-06	-1.07	0.990	10.86	5E-07	0.912	1000
BEC	7.63	0.89	0.997	0.011	11.45	8.77	0.948	1.6E-05	-1.01	0.958	8.32	5E-07	0.699	1000
VSC	8.93	0.58	0.999	0.017	15.72	6.41	0.971	1.3E-04	-1.65	0.976	9.79	1E-06	0.718	707.11
MOC	10.75	2.02	0.999	0.005	13.36	13.5	0.980	2.0E-07	-0.86	0.983	11.13	3E-07	0.878	1291

E. Polymer Adsorption Kinetics Results

Pseudo-first order kinetics, pseudo-second order kinetics, Elovich kinetics and Intraparticle diffusion plots for colour removal were shown in Fig.14-17. The kinetic constant for the four kinetic models are summarized in Table 4. The correlation coefficients for the models were relatively low as compared with those for the pseudo-second order model and also the experimental data shows a good agreement with the pseudo second-order kinetic model data, with the lowest normalized standard deviation, Δq (%) values ranging between 0.96% and 3.15%. The fitting of pseudo-second order kinetic model with high coefficient of determination ($R^2 > 0.993$) further validates coagulation-flocculation process as a second-order process. Elovich model agreement also gave a further insight to the adsorption-chemisorption process. This suggested that the overall rate of the adsorption process was controlled more by chemisorption which involved valence forces through electrons sharing between the polymer and contaminant. Intraparticle diffusion kinetic model is not the sole rate determining step because the linear plot did not pass through the origin [35].
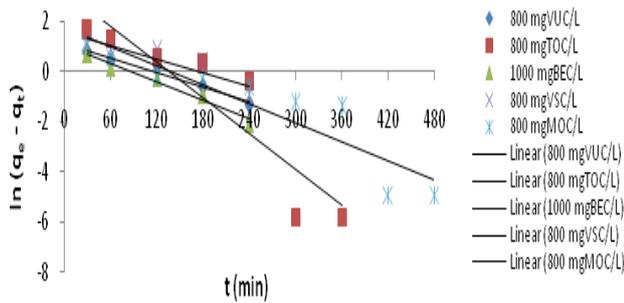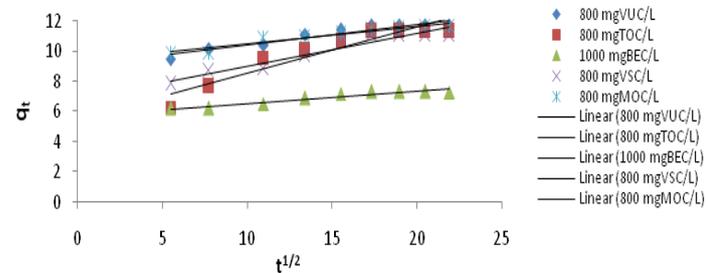

Fig 14. Psuedo –first order Kinetics for the colour removal from AR 44 dye at different coagulants and dosages.
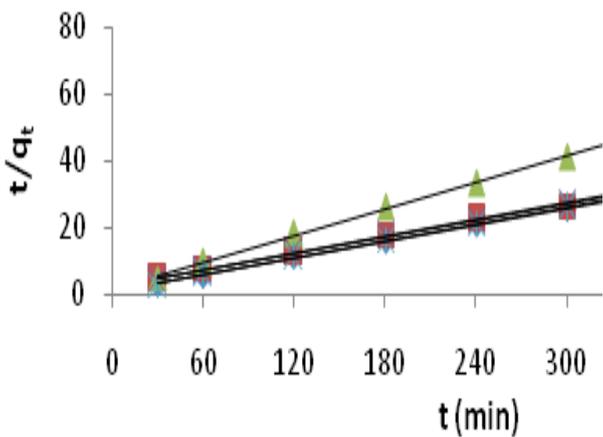
Fig 15. Psuedo –second order Kinetics for the colour removal from AR 44 dye at different coagulants and dosages.
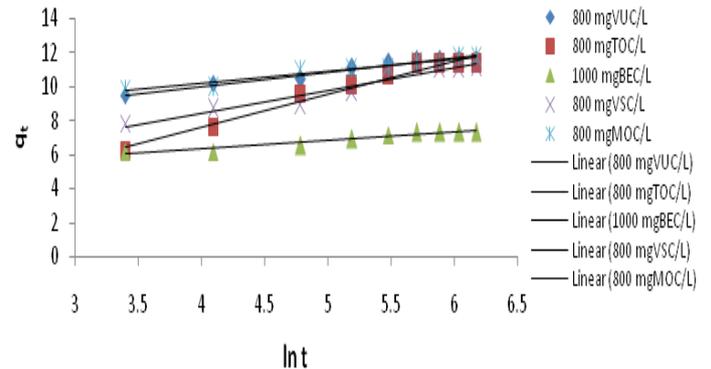
Fig 16. Elovich kinetic model for the colour removal from AR 44 dye at different coagulants and dosages.

Fig 17. Intrparticle diffusion model for the colour removal from AR 44 dye at different coagulants and dosages.

IV. CONCLUSION

Present study analyzed the feasibility of colour removal from acid red 44 using natural organic polymers as coagulants. The coagulants studied have been found to be highly effective in the decolourization process. Operational parameters studied (pH, coagulant dosage, dye concentration, settling time and temperature) influence the colour removal process. Adsorption mechanism is a very important mechanism in the coagulation-flocculation process using natural (plant-based) coagulants. Charge neutralization, sweep-flocculation and interparticle bridging play an important role in enhancing colour removal process.

REFERENCES

[1] G. Zhu, H. Zheng, Z. Zhang, T. Tshukudua, P. Zhang, X. Xiang, Characterization and coagulation-flocculation behaviour of polymeric aluminium ferric sulphate (PAFS), Chemical Engineering Journal. 178 (2011) 50-59.

[2] A. Anouzla, Y. Abrouki, S. Souabi, M. Safi, H. Rhbal, Colour and COD removal of disperse dye solution by a novel coagulant: Application of statistical design for the optimization and regression analysis, Journal of Hazardous Materials. 166 (2009) 1302-1306.

[3] J. Beltrán-Heredia, J. Sanchez Martin, A. Delgado-Regalado, C. Jurado-Bustos, Removal of Alizarin Violet 3R (anthraquinonic dye) from aqueous solutions by natural

coagulants, Journal of Hazardous Materials. 170 (2009) 43-50.

[4] J. Beltran-Heredia, J. Sanchez-Martin, M. A. Davila-Acedo, Optimization of the synthesis of a new coagulant from a tannin extract, Journal of Hazardous materials. 186 (2011) 1704-1712.

[5] B. Bolto, J. Gregory, Organic polyelectrolytes in water treatment, Water Res. 41(2007) 2301-324.

[6] M.G. Antov, B. Marina, N. J. Petrovic, Proteins from common bean (Phaseolus vulgaris) seed as a natural coagulant for potential application in water turbidity removal, Bioresource Technology. 101 (2010) 2167-2172.

[7] S.S.D. Mariângela, O. C. André, M. G. Valdirene, Purification and molecular mass determination of a lipid transfer protein exuded from Vigna unguiculata seeds, Biol plant. 44 (2003) 417-421.

[8] A. Kuku, U.J. Etti, I. S. Ibironke, Processing of fluted pumpkin seed, Telfairia occidentalis (Hook F) as it affects growth performance and nutrient metabolism in rats, Plant Physiol. Biochem. 39 (2014) 137-146.

[9] O.J. Ikegwu, N. U. Oledinmma, V. N. Nwobasi, I. C. Alaka, Effect of processing time and some additives on the apparent viscosity of 'achi' Brachystegia eurycoma flour, Journal of food Technology. 7 (2009) 34-37.

[10] F.J. Massawe, S. S. Mwale, S. N. Azan-Ali, J. A. Roberts, Breeding in Bambara groundnut (Vigna subterranean): strategic considerations, African J. of Biotechnology. 4 (2005) 463-471.

[11] A. Ndabigengesere, K. S. Narasiah, B. G. Talbot, Active agents and mechanism of coagulation of turbid waters using Moringa oleifera, Water Res. 29 (1995) 703-710.

[12] I.A Obiora-Okafo, M. C. Menkiti, O. D. Onukwuli, Utilization of response surface methodology and factor design in micro organic particles removal from brewery wastewater by coagulation /flocculation technique, Inter. J. of Appl. Sci. and Maths. 1(2014) 15 – 21.

[13] A.O.A.C., Official Methods of Analysis 15th Edition, Association of Official Analytical Chemists. Washington D. C, U.S.A. 1990.

[14] T. Okuda, A.U. Baes, W. Nishijima, M. Okada, Improvement of extraction method of coagulation active components from Moringa oleifera seed, Water Res. 33 (1999), 3373-3378.

[15] A. Ndabigengesere, K. S. Narasiah, B.G. Talbot, Active agents and mechanism of coagulation of turbid waters using Moringa oleifera, Water Res. 29 (1995) 703-710.

[16] Z.Z. Abidin, N. Ismail, R. Yunus, I.S. Ahamad, A. Idris, A preliminary study on Jatropha curcas as coagulant in wastewater treatment, Environ. Technol. 32 (2011) 971-977.

[17] J. Eastoe, J.S. Dalton, Dynamic surface tension and adsorption mechanisms of surfactants at the air water interface, Adv. J. Colloid Interface Sci. 85 (2000) 103-144.

[18] I. Langmuir, The adsorption of gases on plane surface of glass, mica and platinum, J. of Ame. Chem. Soc. 40 (1918) 1361-1403.

[19] H.R. Hall, L.C. Eagleton, A. Acrivos, T. Vermeuten, Pore and solid diffusion kinetics in fixed bed adsorption under constant pattern conditions, I and EC fundamentals. 5 (1996) 212 - 223.

[20] H. Freundlich, Colloid and capillary chemistry, Mathuen, London. (1926) 110 - 134.

[21] G. Roop, G. Meenakshi, Activated carbon adsorption; adsorption Energetic, Models and isotherm Equations, Taylor and Francis Group. (2005) 120.

[22] M.J. Temkin, V. Pyzhev, Recent modifications to Langmuir isotherms, Acta Physiochem URSS. 12 (1940) 217–222.

[23] M.M. Dubinin, L. V. Radushkevich, The equation of the characteristic curve of the activated charcoal, Proc. Acad. Sci. USSR Phys. Chem. Sec. 55 (1947) 331–337.

[24] T. Zhang, Q. R. Li, Y. Liu, Y. L. Duan, W.Y. Zhang, Equilibrium and kinetics studies of fluoride ions adsorption on FeO_2/Al_2O_3 composites pre-treated with non-thermal plasma, Chem. Eng. J. 168 (2011) 665 – 671.

[25] S. Lagergren, B. K. Svenska, About the theories of so-called adsorption of soluble substances, Kungsven Velenska-Psad. Hand. 24 (1898) 1 – 6.

[26] Y. S. Ho, G. Mc Kay, Pseudo-second-order model for sorption processes, Process Biochem. 34 (1999) 451 – 465.

[27] A. Khated, A.E. Nemr, A. El-Sikaily, O. Abdelwahab, Removal of Direct N-Blue 106 from artificial textile dye effluent using activated carbon from orange peel: adsorption isotherm and kinetic studies, J. Hazard. Mater. 165 (2008) 100 - 110.

[28] C. Aharoni, F.C. Tompkins, In: Eley D. D, Pines H, Weisz P. B. (Eds.). Adv. Catal. Related Subj., Academic Press, New York, (1970) 21.

[29] W.J. Weber, J. C. Morris, Kinetics of adsorption on carbon from solution, J. Saint. Eng. Div. Proceed. Am. SOC. Civil Eng. 89 (1963) 31 - 59.

[30] V. Vimonses, S. Lei, B. Jin, C. W. K. Chow, C. Saint, Adsorption of Congo red by three Australian Kaolins, Appl. Clay Sci. 43 (2009) 465 – 472.

[31] G.H Jeffrey, J. Bassat, J. Mendham, R. C. Denney. Textbook of quantitative chemical analysis, Fifth Edition. Longman Scientific & Technical. (2005) 649-720.

[32] G. Li, J. Gregory, Flocculation and sedimentation of high turbidity waters, Water Res. 25 (1991) 1137-1143.

[33] S.S. Moghaddam, M.R. Alavi Moghaddam, M. Arami, Coagulation/flocculation process for dye removal using sludge from water treatment plant: optimization through response surface methodology, Journal of Hazardous Materials. 175 (2010) 651-657.

[34] B.H. Hameed, D.K. Mahmoud, A.L. Ahmad, Equilibrium modelling and kinetic studies on the adsorption of basic dye by a low-cost adsorbent: Coconut (Cocos nucifera) bunch waste, J. Hazard. Mater. 158 (2008) 65 - 72.

[35] M. Ozacar, I.A. Engil, H. Turkmenler, Equilibrium and kinetic data, adsorption mechanism for adsorption of lead onto valonia tannin resin, Chem. Eng. J. 143 (2008) 32 – 42.

APPENDIX

Table 4.Adsorption kinetics model parameters for colour removal from AR 44 dye.

Dye	Coagulants dosages (mg)	Pseudo-first-order kinetics					Pseudo-second-order kinetics					Elovich kinetics		
		q_e, exp (mg/g)	q_e, cal (mg/g)	K_{F1} (min^{-1})	R^2	Δq (%)	q_e, cal (mg/g)	K_2 (g/mg min)	R^2	h (mg/g min)	Δq (%)	a	b	R^2
AR 44	800 mgVUC/L	11.68	4.78	0.009	0.963	20.88	12.05	0.0887	0.999	12.88	1.12	2214.9	1.183	0.965
	800 mgTOC/L	11.34	24.78	0.023	0.823	41.9	12.35	0.0303	0.999	4.62	3.15	1.843	0.518	0.971
	1000 mgBEC/L	7.3	1.95	0.01	0.911	25.91	7.52	0.0836	0.999	4.73	1.07	3362.8	2.028	0.925
	800 mgVSC/L	11.1	4.899	0.009	0.851	19.75	11.76	0.0395	0.997	5.46	2.1	14.77	0.759	0.933
	800 mgMOC/L	11.73	4.78	0.012	0.824	20.95	12.05	0.0853	0.999	12.39	0.96	21368	1.404	0.953

Table 5 Intraparticle parameters for the polymer adsorption mechanism for colour removals from AR 44 dye.

Dye	Coagulants dosages (mg)	Intraparticle diffusion		
		C	K_{id} (mgg^{-1} min$^{1/2}$)	R^2
AR 44	800 mgVUC/L	9.059	0.135	0.912
	800 mgTOC/L	5.489	0.305	0.899
	1000 mgBEC/L	5.731	0.08	0.914
	800 mgVSC/L	6.862	0.216	0.924
	800 mgMOC/L	9.337	0.116	0.934